

CHAPTER 3

PRODUCTION OF NANOFIBRILLATED CELLULOSE FROM LIGNOCELLULOSIC WASTES USING SYNTHESIZED GREEN SOLVENTS AND HIGH INTENSITY ULTRASONICATION AND ITS CHARACTERIZATION STUDIES

3.1 Introduction

The present study focuses on the valorisation of SCB for the sustainable production of NFC. SCB is an abundant lignocellulosic by-product in many regions and, aside from its use in co-generation, is largely underutilized. Its surplus availability, low pre-processing and transportation costs, and potential for economic returns during off-seasons make it an ideal candidate for high-value product development. A critical step in this process is the deconstruction of the complex lignocellulosic matrix of SCB, enabling the separation of its primary constituents: cellulose, hemicellulose, and lignin [141]. Efficient fractionation is essential for the subsequent valorisation of cellulose and other biomass components. Conventional methods for NFC production from lignocellulosic biomass including acid/alkali treatments and the use of harsh reagents have been widely reported [142][143]. However, these techniques often involve laborious processes, toxic by-products, and environmental concerns. As a result, current research is increasingly geared toward greener, more sustainable alternatives. Among these, green solvents such as ionic liquids, organosolv systems, and DES have gained prominence. Notably, natural deep eutectic solvents, comprising biologically derived components such as organic acids, sugars, choline derivatives, and polyols, have shown strong potential for lignocellulosic biomass fractionation due to their low toxicity, biodegradability, cost-effectiveness, and ease of preparation [130].

Acidic NADES, formed from combinations of carboxylic acids (e.g., oxalic, citric, tartaric acids) and polyols (e.g., glycerol, xylitol, ribitol) in equimolar ratios, have demonstrated notable efficiency in the dissolution of hemicelluloses and partial delignification [144,145][146]. However, to obtain pure cellulose fibres, it requires complete delignification. To address this, an organosolv treatment was integrated as a second step. Organosolv processes especially acetosolv involving aqueous acetic acid (60–90% v/v) supplemented with minor quantities of hydrochloric acid (0.25–0.5% v/v) facilitate effective delignification by enhancing lignin solubility into the acetic acid phase [147][148]. Following chemical pretreatment, nanofibrillation was achieved using assistive technique, HIU, a mechanical process that avoids hazardous chemical usage [149,150]. Despite growing interest in green chemistry approaches, the combined application of synthesized NADES, acetosolv delignification, and ultrasonication for NFC production from SCB remains relatively unexplored.

In this study, four different acidic NADES were synthesized using various combinations of citric and tartaric acids with xylitol and glycerol in equal molar ratios, along with water. These were evaluated for their efficiency in biomass fractionation and NFC production under identical reaction conditions. The structural and compositional characteristics of the synthesized NADES were elucidated using ^1H NMR and FTIR spectroscopy. Detailed physicochemical and morphological analyses of the resulting NFCs were conducted using advanced analytical techniques.

3.2 Experimental methodology

3.2.1 Production of NFC

Sugarcane bagasse samples were procured from nearby local market and used as cellulosic precursor material for nanocellulose fabrication. The obtained samples were

sorted, cleaned, and de-pithed manually. The collected feedstock was sun-dried under ambient environmental conditions over a period of 7 days and cut into small pieces (1-2 cm). The dried and cut bagasse was ground into smaller fractions and passed through 60 mesh (≤ 0.25 mm screen size). The ground bagasse was again washed with acetone (1:10 w/v) to eliminate dirt and other extractives.

3.2.2 Synthesis of NADES

For the pre-treatment process of lignocellulosic biomass namely sugarcane bagasse, four different types of NADESs; glycerol-citric acid, xylitol-citric acid, glycerol-tartaric acid and xylitol-tartaric acid were prepared by mixing with water at fixed molar ratios i.e., 1:1:10 with continuous stirring and heating at 75 - 80°C to obtain a clear and viscous liquid. The synthesized NADES were designated as Gly-CA, Xyl-CA, Gly-TA and Xyl-TA for clarity. The pH of the NADESs were determined using a pH meter (IKON, India).

3.2.3 High intensity ultrasonication assisted two-stage cascade process

The depolymerization of feedstock biomass is the main challenge in the recovery of cellulose fibres from biomass for subsequent production of NFC [151]. It comprises two stage production process. The first stage process mainly includes two sequential steps; the first step is pretreatment step using green solvents that mainly involves hemicellulose solubilization, delignification and cellulose recovery. The second stage includes production of NFC using HIU.

3.2.3.1 Pretreatment of biomass (cellulose recovery)

The first step comprised of pre-treating the biomass samples using combination of NADES and acetosolv. Four biomass pretreatment experiments were carried out

individually by using synthesized NADESs in 1:10 (feed solvent ratio). A round-bottom flask containing 10 g of extractive-free ground bagasse and 100 mL of NADES was placed in an oil bath maintained at 100 °C temperature. The mixture was refluxed for 2 hours with a stirring speed of 150 rpm. Afterward, the flask was taken out of the oil bath and the resulting slurry was subjected to vacuum filtration to separate NADES-treated solid residue and solubilized hemicellulose fractions. The supernatant was collected and cold ethanol was added to it. This was done to recover NADES from the mixture. The mixture was subjected to centrifugation, resulting in the separation of the supernatant liquid mixture containing ethanol (used as an anti-solvent) and NADES. The separation was achieved via vertical distillation columns maintained at a temperature of 80 °C. The distinct boiling temperatures of the components made this separation feasible. Ethanol was obtained at the top while NADES was collected at the bottom part. The recovered NADES and ethanol were subsequently reused in the process.

The obtained solid residue in the second step was delignified using clean fractionation technique i.e., acetosolv method. The residue was mixed with 30 mL of aqueous acetic acid (60% v/v) and hydrochloric acid (0.4% v/v) and heated to boiling point (114 °C) in a round bottom flask under atmospheric pressure. The process was carried at total reflux with stirring for 2 h. Following the completion of the reaction, the mixture was subjected to centrifugation at 10,000 rpm for 15 min for separation. The residual cellulose slurry was first washed with dil. acetic acid to avoid any lignin deposition on the samples and then multiple times with cold distilled water until neutral. Additional water washing and repeated screening helped in obtaining high state of pure cellulose. The extracted cellulose was let dry at 60 °C overnight.

3.2.3.2 Conversion of cellulose fibres to nanofibrillated cellulose

The isolated cellulose fibres were suspended in ethanol and subjected to HIU using digital ultrasonicator (Toshcon India, ultrasonic power supply: 20 kHz, consumption power: 650 W, pulse of 15/15 sec on/off) to obtain NFC. Ultrasonication process was performed for 30 min at 30 °C. Afterward, each of the suspensions were centrifuged at 10,000 rpm for 15 min. For convenience, the final products were named with respect to the utilized NADESs; NFC/Gly-CA, NFC/Xyl-CA, NFC/Gly-TA and NFC/Xyl-TA. The ethanol was recovered and reused. The produced NFCs were stored for further characterization and future application. Figure 3.1 shows the schematic representation of the process design of the experiment, illustrating various unit operations.

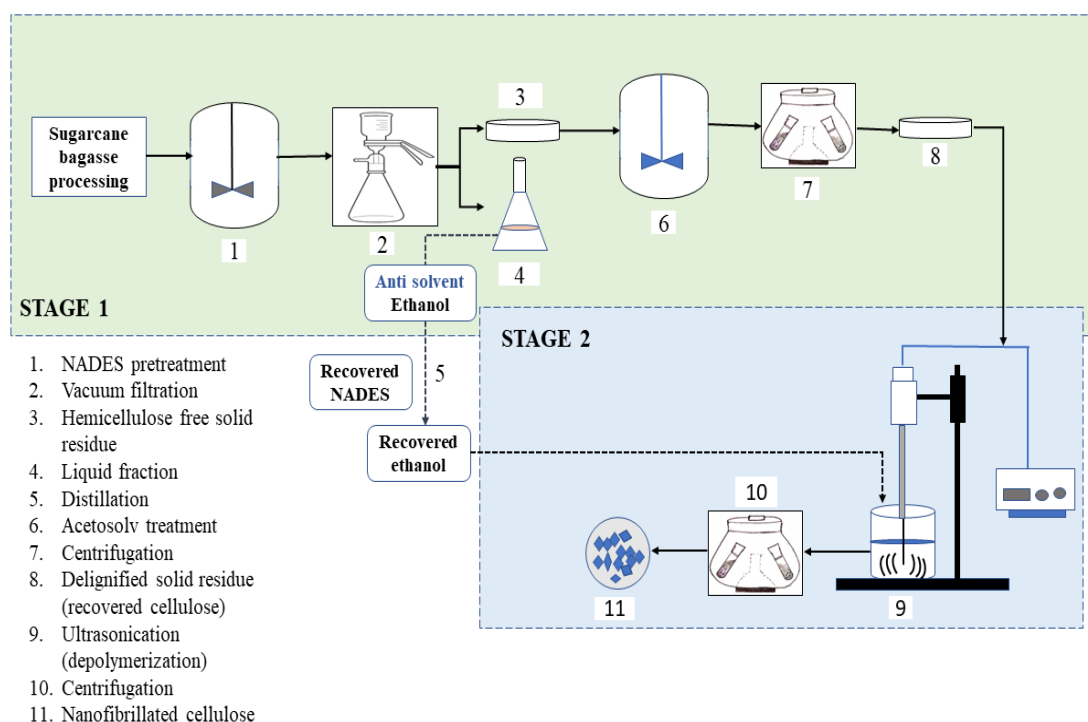


Figure 3.1 Schematic representation of experimental design of nanofibrillated cellulose production.

3.3 Synthesis of NADES

Four different precursors used to synthesize NADES resulted in the formation of clear and homogenous liquids, without any precipitates when kept at ambient temperature. Eutectic solvents are formed through the combination of hydrogen bonding between the precursor molecules, as well as intermolecular interactions that involve Van der Waals forces and electrostatic forces [152]. During preparation of NADES, water was also added to the mixture as this resulted in reduction in the viscosity of NADESs, smaller preparation time, and reaction temperature. The decrease in viscosity facilitates improved solvent penetration into the biomass and enables easier disruption of its structure [153]. Savi and his team worked on synthesis of NADES and concluded that NADES can incorporate water into their structure without compromising their functionality, which leads to a decrease in both the time and temperature required during its synthesis process [154]. In one study conducted by Panyamao and his co-workers concluded that the pretreatment involving NADESs-water system positively influenced the dissociation of hemicellulose and lignin rather than the solubilization of cellulose [155]. In another study, the addition of water to the synthesized (DES) demonstrated to have a vital and beneficial impact on the extraction of cellulose, hemicellulose and lignin from chestnut shell wall [144].

The pH values of all the synthesized NADES were determined and the exhibited values ranged from 3.5 ± 0.5 . Biomass pretreatment is also influenced by the pH level, where pH values below 7 leads to complete solubilization of hemicelluloses, further reducing the requirement for any enzymatic breakdown [156]. Figure 3.2 represents the FT-IR analysis of synthesized NADES as well as of the precursor materials (initial reagents) that display specific bands corresponding to the functional groups present in the

precursor molecules used. Both the IR data revealed the preservation of characteristic bands corresponding to the constituent materials and affirmed the successful synthesis of NADES.

3.3.1 FT-IR of synthesized NADES

The FTIR spectra presented in Figure 3.2 exhibit distinctive bands associated with the functional groups of the precursor materials used in the synthesis of the NADES. The absorption spectrum of citric acid displayed a peak at 3500 cm^{-1} , indicating stretching vibrations of free hydroxyl (-OH) groups within the molecule [157]. Additionally, characteristic bands were observed at 1660 and 1750 cm^{-1} , which were attributed to the stretching vibrations of C=O and C-O-H bonds, respectively [158]. Tartaric acid presented absorption bands within the range of 1700 to 3600 cm^{-1} in the infrared spectrum that correspond to the stretching vibrations of OH, CH, and C=O bonds exhibiting distinctive characteristics in terms of their shape and frequency [159].

All the four NADES exhibited a prominent absorption band ranging from 3330 to 3600 cm^{-1} , indicating the stretching vibrations of the hydroxyl (-OH) groups [157]. In addition, an absorption band at 1660 cm^{-1} was observed, which could be ascribed to the angular deformation of hydroxyl groups of water molecules existing in NADES. Irrespective of precursors used in synthesis, the absorption band associated with C=O stretching in all NADES showed a transposition towards higher wavelengths compared to the spectra of the precursor reagents. This transposition indicated the rise in electron density on the carbonyl oxygen atom which could be inferred by generation of hydrogen bonds in the solvent.

As seen in Figure indicated by arrow marks, the spectra of Xyl-CA compound displayed a change in the C-O band position, shifting from 1690 to 1750 cm^{-1} , signifying the

presence of hydrogen bonds formed between the precursor molecules. Additionally, the νOH absorption band showed a relocation towards lower wavenumbers, specifically within the range of 1900 to 2600 cm^{-1} , providing further confirmation of formation of hydrogen bond between the starting compounds [152]. Furthermore, the other NADES also exhibited displacement in the C-O band towards higher wavenumbers and the -OH band towards lower wavenumbers. Also, the absorption spectrum of all the acidic NADESs exhibited C-H bonding in the range of 700 – 1600 cm^{-1} , which can be attributed to the chemical structure of hydrogen bond donors (HBD) (citric acid and tartaric acid here) [160]. Thus, the FTIR spectra not only enabled to determine the functional groups present in the precursor materials, but also provided evidence of possible changes in structure caused by intermolecular interactions such as Van der Waals and electrostatic forces occurring between the initial reagents used in the synthesis of eutectic solvents.

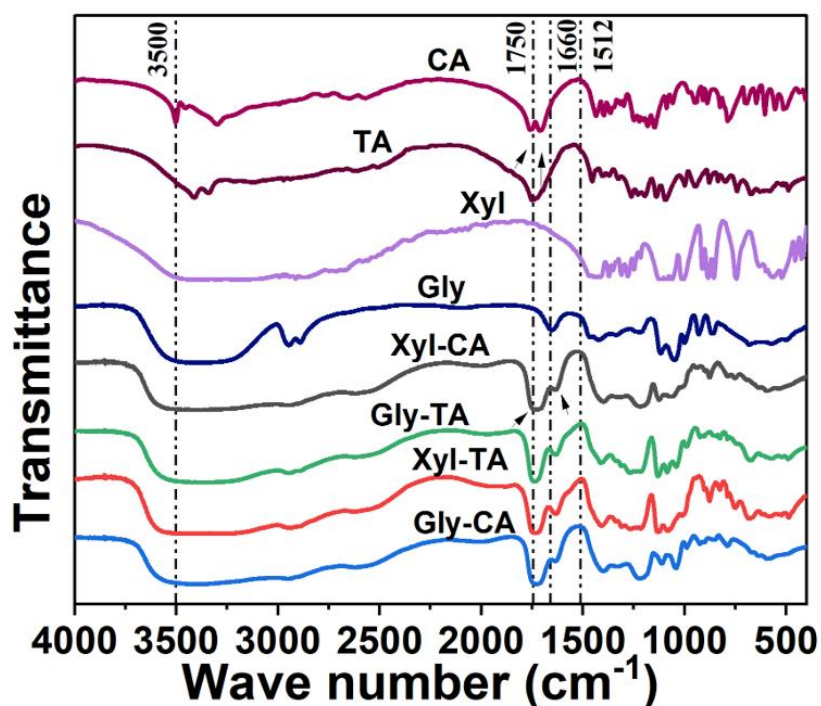


Figure 3.2 FT-IR analysis of synthesized NADES and their individual components.

3.3.2 Nuclear magnetic resonance (^1H NMR)

To explore the supermolecular structure of NADES, the eutectic solvents were locked with deuterium oxide and the resulting mixture was subjected to NMR analysis. Figure 3.3 displays the NMR spectra of the individual components and synthesized NADES that were employed in the synthesis of NADES. The ^1H NMR integration results confirmed the equimolar ratio of individual components in the NADES i.e., 1:1. Also, by comparing the NMR signals, it was found that the distinct peaks of glycerol, xylitol, citric acid and tartaric acid persisted in the ^1H NMR spectrum of the synthesized NADES and presence of no new peaks reveal that no other compounds were formed. The distinctive signal of NADES protons exhibited a slight upfield shift in comparison to the protons in free glycerol, xylitol, citric acid, and tartaric acid. These upfield chemical shifts are indicative of the formation of hydrogen bonds in the NADES. Hydrogen bonding shifts the resonance signal of a proton to lower field i.e., to higher frequency [161]. The intermolecular interactions between the components of NADES may have impacted the electron density surrounding the protons, leading to alterations in these chemical shifts of the protons. For instance, in the Gly-CA NADES system, slight deviation in chemical shift can be observed in the characteristic peak of glycerol structure, peak value, $\delta = 3.76, 3.64$ and 3.54 ppm shifted to $3.63, 3.50$ and 3.42 ppm while for citric acid structure from 2.95 and 2.77 ppm to 2.89 and 2.71 ppm respectively. In Xyl-CA, peak value, δ of xylitol $3.80, 3.71$ and 3.64 ppm shifted to $3.70, 3.61$ and 3.54 ppm respectively while peak value of citric acid shifted to 2.93 and 2.75 ppm in the synthesized system. In Gly-TA NADES, peak value, $\delta = 3.76, 3.64$ and 3.54 ppm shifted to $3.67, 3.53$ and 3.45 ppm and for tartaric acid, the characteristic peak value marked a chemical shift from 4.68 ppm to 4.64 ppm. In Xyl-TA, peak value, δ of xylitol

3.80, 3.71 and 3.64 ppm shifted to 3.69, 3.61 and 3.53 ppm respectively while peak value of tartaric acid shifted to 4.64 ppm. Thus, the NMR study confirms that the signal of the molecular group from individual components matched the corresponding position in the NMR spectrum of the NADES, indicating its high purity. The surplus hydroxyl group in NADES was not discernible in the spectrum, likely due to the rapid exchange of protons from NADES with the D₂O solvent. In the present study, the addition of water in NADES formulation does not alter the structure of NADES as the NADES were synthesized using only 10 mol of water (i.e., approximately 36% v/v). In a study conducted by Dai and his co-workers, it was observed that the supramolecular complex structures of synthesized NADES remain unaltered when the water content is less than 50% [162].

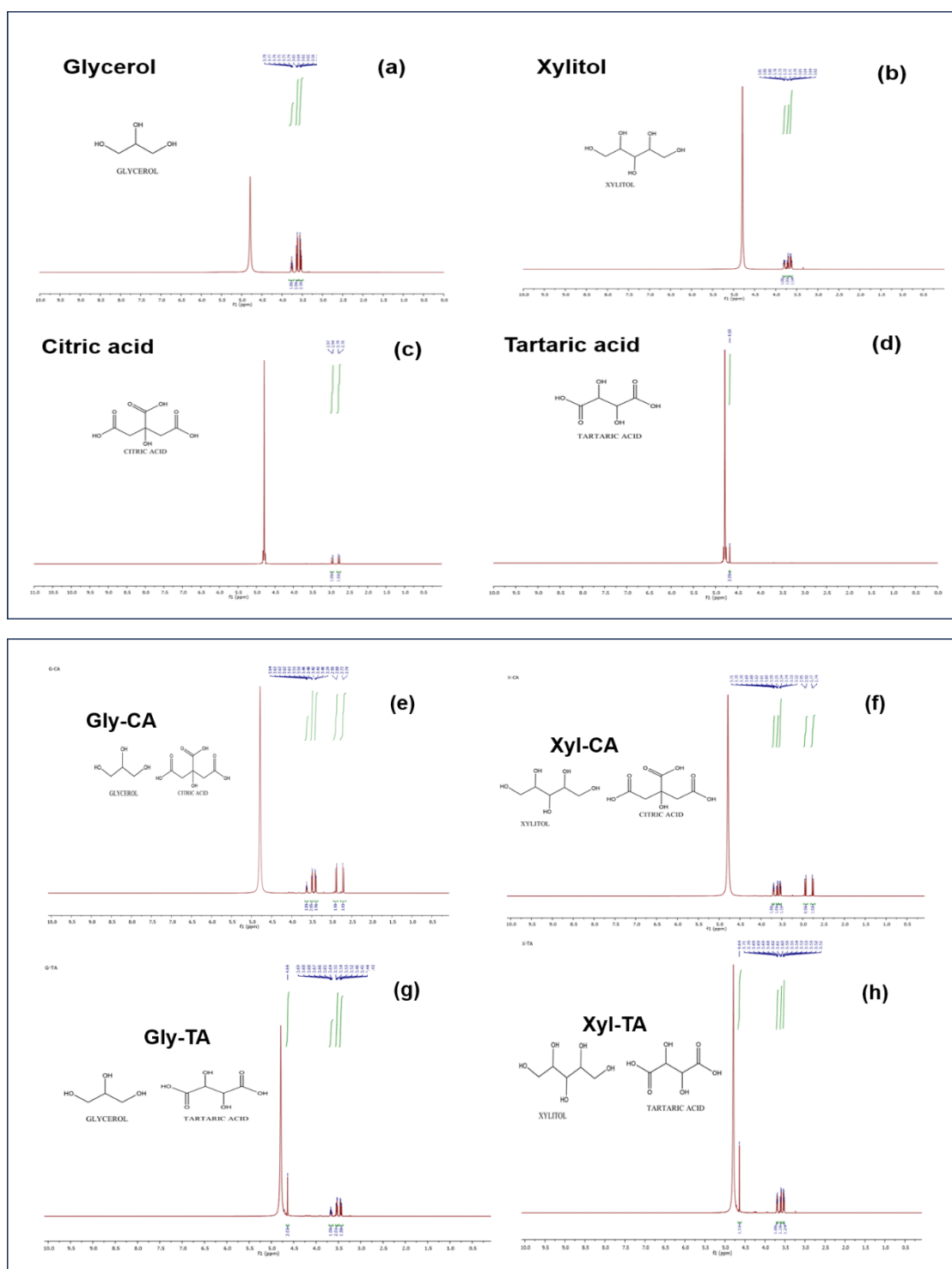


Figure 3.3 ^1H NMR spectra of (a) Glycerol; (b) Xylitol; (c) Citric acid; (d) Tartaric acid; (e) Gly-CA; (f) Xyl-CA; (g) Gly-TA; (h) Xyl-TA.

3.4 Compositional analysis of raw SCB

The compositional analysis of SCB (sugarcane bagasse) revealed approximately 45 ± 0.2 % of cellulose content, 35 ± 0.8 % of hemicellulose, lignin content of approximately 14 ± 0.5 %, along with smaller amounts of ash (1.5 – 2.5 %) and other extractives (3 – 4 %). Despite the variation in geographical origin, the composition of biomass falls within the range reported in the literature [163,164].

3.5 Experimental design of NFC production

Lignocellulosic biomass (LCB) is recalcitrant structure that stems from the complex interaction of cellulose, hemicellulose, and lignin. Prior to conversion of LCB into new value-added products, these complexes required pretreatment i.e., fractionation or deconstruction into its individual components. This can be achieved by mild or diluted acids as they are very effective

in biomass solubilization [165]. Hence, acidic NADES and acetosolv solvents are more suitable options in the defragmentation of LCB. First and second step in this first stage of process comprises cellulose recovery. It consists of pretreatment of SCB for hemicellulose solubilization using different NADES and then delignification of the residual fraction using acetosolv solvent in a sequence.

The maximum yield of cellulose was approximately around 0.38 ± 0.02 g/g of SCB (84.4 %) which was obtained with combined Gly-CA (NADES) and acetosolv treatment and on depolymerization resulted in 0.36 ± 0.02 g of NFC per g of SCB (80 %). Table 3.1 depicts the total cellulose recovery from SCB and subsequent NFC production after depolymerization of cellulose. NADES Xyl-CA resulted in 82.2 % cellulose recovery followed by 76 % for Gly-TA and 69 % for Xyl-TA treatment

methods. The higher cellulose recovery from citric acid-based NADES is likely due to its strong acidity and chelating ability, which effectively disrupt lignin–carbohydrate complexes. This enhances delignification and facilitates easier cellulose extraction from lignocellulosic biomass [166][167,168]. After the hemicellulose separation process, the resulting filtrate underwent distillation. The distillation process yielded ethanol as the distillate, which was utilized for precipitation, while NADES was obtained as the bottom product. This particular stage of process led to successful recovery of 75 % of NADES and 88 % of ethanol. The recovered NADES exhibited a mild peach colour, attributable to the presence of trace amounts of lignocellulosic biomass components. In contrast, the fresh solvent was transparent in colour. Delignification is primarily accomplished using organic acid (clean) fractionation [165]. In case of SCB, short chain fatty acids such as acetic and formic acid have been used as biomass fragmentation owing to their good delignification selectivity [169,170]. Various catalysts like very dil. HCl, H₂SO₄ and H₂O₂ are only added to assist the delignification process [170]. The acetic acid catalysed pretreatment involves following significant chemical reactions; cleaving β -O-4 linkages in lignin, lignin condensation, hydrolysis of ester bonds, and esterification of hydroxyl (-OH) groups. The dissolved lignin obtained from acetic acid fractionation usually obtains more acetyl groups in the C α and C γ positions, inferring both cleavage of ester linkages and the acetylation of lignin during the process [165]. This step helps to remove lignin adequately without causing significant degradation of cellulose fibres.

Second stage is the depolymerization stage in which the extracted cellulosic residue is converted to nanofibrillated cellulose. This step is essential as it provokes the formation of nanoscale cellulose. In this stage, each pretreated cellulose was suspended in ethanol

and exposed to nanofibrillation treatment using HIU. The ultrasonic cavitation led to the disintegration of cellulose and production of NFCs. Since this stage was similar for all the production process, therefore not much difference was noticed in the NFC production percentage from extracted cellulose. Gly/CA treatment of sugarcane bagasse resulted in the highest NFC yield of 84.4 % due to the maximum cellulose extraction achieved through pretreatment.

Following the pretreatment, all NFCs suspensions remained stable without any noticeable precipitation. This outcome suggests that NFCs possess smaller sizes, enabling them to be evenly dispersed within the suspension. Ethanol was recovered and reused for further experiments. The application of intense ultrasonication in the production of fibrillated nanoparticles has considerably expanded their potential applications, especially in biomedical

fields like tissue engineering, medical implants and delivery of bioactive molecules and wastewater treatment [171,172]. Furthermore, they show significant potential in the development of cementitious composites, enhancing both mechanical strength and barrier properties [173].

Table 3.1 Acid-catalyzed recovery of cellulose and total NFC production from SCB.

S. no.	NFCs	Cellulose recovery (g/g of SCB)	NFC production (g/g of cellulose)	Total NFC production (g/g of SCB)
1.	NFC/Gly-CA	0.38 ± 0.02	0.95 ± 0.01	0.36 ± 0.02
2.	NFC/Xyl-CA	0.37 ± 0.02	0.94 ± 0.01	0.34 ± 0.02
3.	NFC/Gly-TA	0.34 ± 0.02	0.93 ± 0.01	0.31 ± 0.02
4.	NFC/Xyl-TA	0.31 ± 0.02	0.94 ± 0.01	0.29 ± 0.02

3.6 Characterizations and analysis of NFCs

3.6.1 Fourier Transform Infrared Spectroscopy (FT-IR)

FT-IR analysis was conducted to investigate the presence of specific functional groups in NFC as well as pure cellulose samples (Figure 3.4 a). The presence of cellulosic functional groups in the NFC samples was confirmed by characteristic absorption peaks observed at $3600 - 3000 \text{ cm}^{-1}$, 2900 cm^{-1} , 1665 cm^{-1} , 1435 cm^{-1} , $1385 - 1375 \text{ cm}^{-1}$, 1150 cm^{-1} , $1060 - 1030 \text{ cm}^{-1}$, 858 cm^{-1} , and 625 cm^{-1} as per the established standard [174] (also observed in pure cellulose samples). The wideband within the range of 3600 and 3000 cm^{-1} indicates alcoholic stretching.

Absorbance peak between 2900 and 2840 cm^{-1} attributes to asymmetric stretching of aliphatic CH_2 groups. The absorbance peaks observed at 1665 cm^{-1} corresponds to the O-H bending mode of absorbed water molecules in cellulosic fibre [157]. The peak located at 1435 cm^{-1} corresponds to the bending of CH_2 groups in cellulose [103]. Additionally, the peak at 1380 cm^{-1} is attributed to the C-H ester band, which arises from partial acetylation of hydroxyl groups found in cellulose. The peaks observed at 1150 cm^{-1} and 1050 cm^{-1} correspond to C-C bending vibration and C-O-C glycoside ether bond of β -1,4-glycosidic ring linkages between the D-glucose units in cellulose for all the NFC samples respectively [175]. The peak at 858 cm^{-1} is the C-H vibration in cellulose that is the characteristic absorption peak of cellulose and has been reported in several studies [176]. The peak located at 625 cm^{-1} attributed to the C-OH out of plane bending in cellulose. The FT-IR analysis confirmed that the samples exhibited structural and functional groups similar to pure cellulosic materials. Notably, the absence of absorption peaks at 1735 cm^{-1} , that indicates C=O stretching associated with

aldehyde, ketone, or carboxylic acid groups in hemicellulose, and the absence of an absorption peak near 1505 cm^{-1} and 1596 cm^{-1} , corresponding to the C=C vibration of the aromatic skeletal structure in lignin, affirmed the effective removal of hemicellulose and lignin from SCB during pretreatment process [177,178]. This further ascertained that FTIR spectra of pure cellulose and the synthesized NFCs exhibited almost similar spectra and the pretreatment steps did not have any significant effect in the synthesis process.

3.6.2 X-ray Diffraction (XRD)

XRD was performed to investigate the degree of crystallinity of nanofibrillated cellulose samples. The diffraction patterns displayed in Figure 3.4 b demonstrate that the crystalline structure of NFCs remained unchanged, and there was no transformation into any other crystalline form during the pretreatment process with natural deep eutectic solvents (NADES), acetosolv solvent and high intensity ultrasonication (XRD pattern of the starting material is reported elsewhere). The peaks observed in all the NFC samples at 2θ values of 16.4° , 22.2° and 34° correspond to the crystallographic planes (110), (200), and (040) of typical cellulose respectively [179]. These peaks are attributed to the cellulose I β structure that confirms the presence of type I natural cellulose form [180]. This indicates that all the cellulose samples did not undergo any dissolution during the pretreatment steps.

Segal's method was employed to calculate the crystallinity index (CrI), which is a crucial parameter affecting the mechanical and thermal properties (equation 2.1). The CrI of nanofibrillated cellulose samples were synchronous to reported NFC samples i.e., $\sim 65\%$. [175,181]. The crystallinity index (CrI) after the nanofibrillation process

were measured as 63.5 %, 62.8%, 60.7% and 60.1 % for NFC/Gly-CA, NFC/Xyl-CA, NFC/Gly-TA and NFC/Xyl-TA, respectively. Overall, these results imply that both natural deep eutectic solvent and acetosolv solvent serve as a mild pre-treatment agent for lignocellulosic biomass defragmentation. However, based on diffractogram peak intensities and CrI values, it is observed that NFCs pretreated with Gly-CA and Xyl-CA (NADES) had much similar CrI values to that of original cellulose CrI values. High crystallinity index specifies an improved toughness of the cellulose structure and mechanical properties. The NFCs synthesized in our study have good crystallinity index and hence, they can be used in many potential applications.

3.6.3 Thermogravimetric Analysis/ Differential Thermogravimetry (TGA/DTG)

When a material is subjected to heat, its structure undergoes changes such as decomposition or phase transitions. Assessing the thermal stability of any material is crucial as it provides insights into the temperature range within which the material can be utilized without experiencing any alterations. The degradation behaviours of nanofibrillated cellulose particles were examined using TGA and DTG and are depicted in Figure 3.4 c and d. The TGA curves indicate changes in mass percentage, representing the degradation of the samples as they are heated sequentially while DTG analysis determines the temperature at which the sample experiences the highest rate of mass loss and evaluates the thermal stability of material. The degradation process of cellulose typically involves three major reactions: dehydration, depolymerization, and glucosans formation [182]. The TGA results for all synthesized NFCs derived from SCB exhibit a similar degradation pattern. Initially, there is a decrease in mass in the temperature range of 35 to 105 °C, which is attributed to the vaporization of surface-bound moisture, whereas the water that was bound by intermolecular hydrogen bonds,

evaporated at temperatures around 120 °C [183]. Depolymerization of cellulose at temperatures ranging from 120 to 280 °C likely occurs through the breakage of β -1,4-glycosidic linkages, accompanied by intramolecular rearrangements of monomeric units, resulting in a maximum mass loss. Subsequently, there is a steep decline up to 380 °C that may be due to release of glucosan monosaccharides, contributing to a total mass loss of approximately ~ 80% (revealed by DTG curve). At temperatures exceeding 600°C, the material undergoes charring as a result of complete combustion, leading to the formation of a residue comprising nearly 20 % of the initial mass. The lower stability of NFC samples particularly NFC/Gly-CA begins to degrade at 248 °C, with its maximum degradation rate occurring at 350 °C (also revealed by DTG curve), can be attributed to factors such as the smaller (nano) size of the samples, greater number of free ends in the polymeric chain, decrease in molecular weight, and degradation of the amorphous regions of cellulose [105].

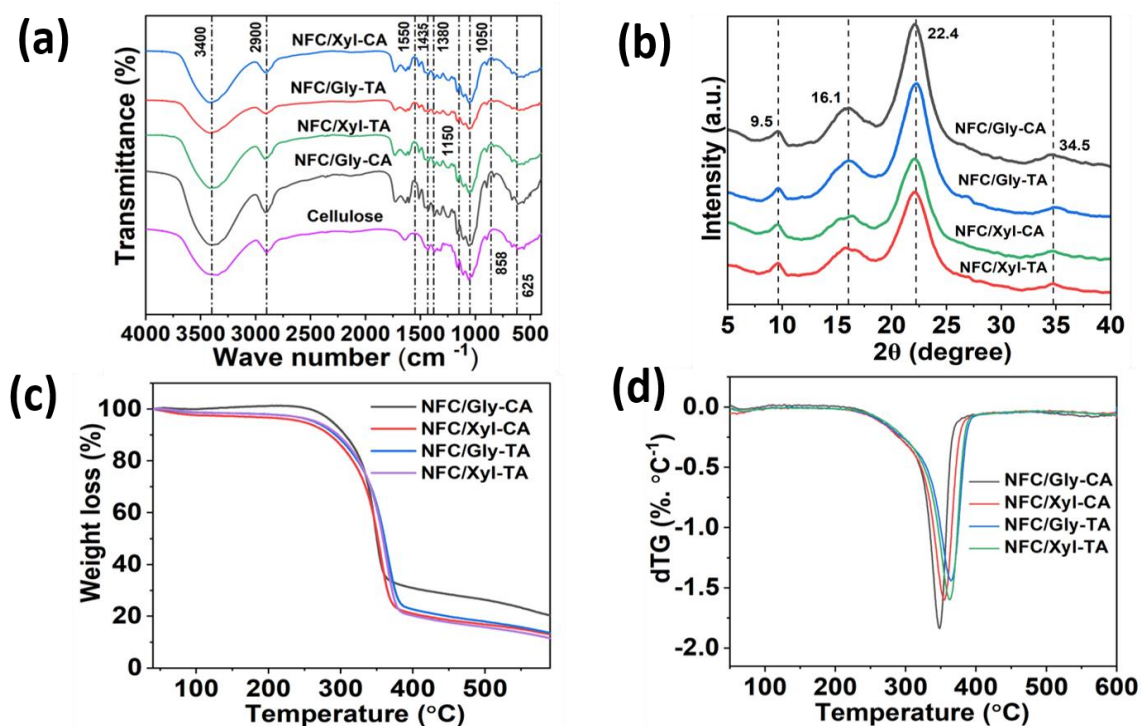


Figure 3.4 (a) FT-IR spectra; (b) XRD analysis; (c) TGA; (d) DTG of NFC samples synthesized using different pretreatment methods.

3.6.4 Dynamic Light Scattering (DLS)

By subjecting the extracted cellulose to an intense ultrasonication process at a frequency of 20 kHz (650 W) for a duration of 30 minutes, a significant reduction in particle size is achieved, resulting in the production of nano-sized particles. The size distribution curve indicated the average particle size of the NFC suspension that were in the range of 15 to 50 nm (Figure 3.5). The average particle size for NFC/Gly-CA and NFC/Xyl-CA were nearly similar i.e., $\sim 30 \pm 5$ nm with Z-average size of 32 ± 2 nm while NFC/Gly-TA and NFC/Xyl-TA showed similar values i.e., $\sim 70 \pm 5$ nm and Z-average value of 45 ± 5 nm. The DLS results validated the depolymerization of cellulose, transitioning it from micron-sized particles to nano scale. DLS is a technique that estimates the Brownian movement of particles in a suspension by analysing the intensity shift of scattered light. This information is then used to determine the diffusion coefficient and size of the particles. The DLS analysis also provides several key parameters for the NFC suspension, including the polydispersity index (PDI), particle size distribution, and average particle size. Polydispersity index (PDI), also referred to as the heterogeneity index, serves as a metric to assess the distribution of molecular mass within a specific polymer sample. The PDI is quantified on a numerical scale, spanning from 0.0 (indicating a perfectly uniform sample in terms of particle size) to 1.0 (representing a highly polydisperse sample with multiple particle size populations). In case of NFC samples, PDI was less than or equal to 0.5, which is considered admissible for polymeric nanomaterials [184].

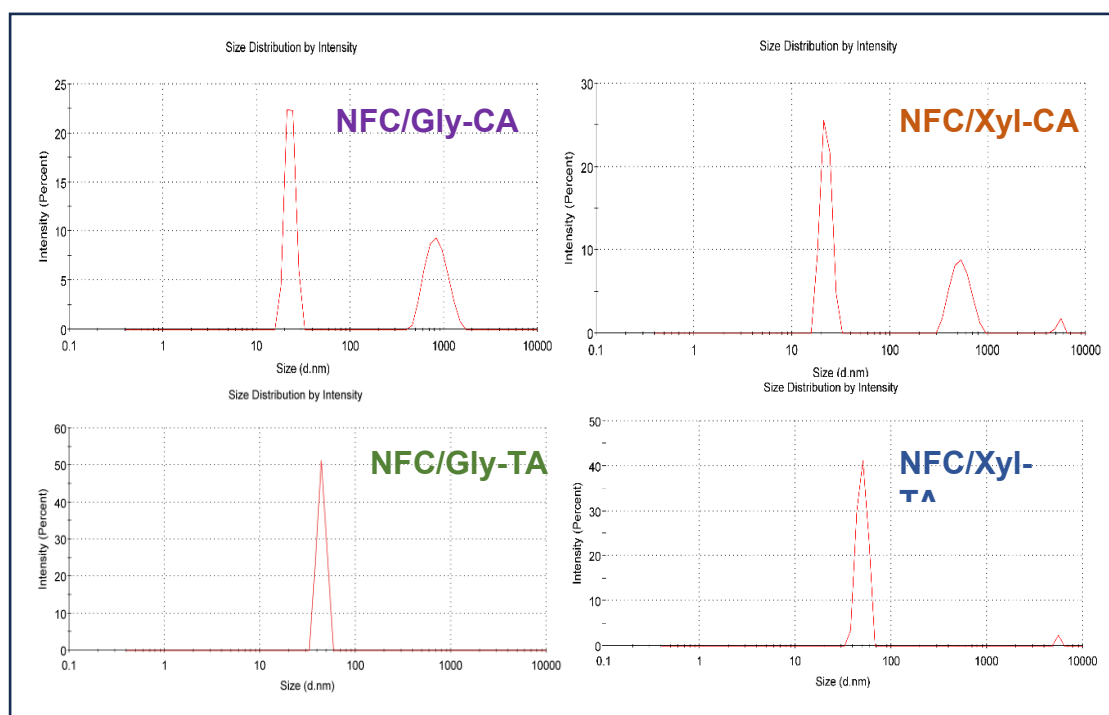


Figure 3.5 Particle size distribution of synthesized NFCs.

3.6.5 Transmission Electron Microscopy (TEM)

The TEM micrographs presented in Figure 3.6 provides an additional insight into the effect of pretreatment steps and size of the NFCs produced from SCB. TEM analysis of citric acid-based NADES treatment was analysed due to its high efficiency in disintegrating the biomass. As visualized, the NFCs comprise a typical tangled web-like arrangement of nanofibrous structure, exhibiting high aspect ratio. The particle size analysis through imageJ software revealed that NFCs prepared in our study illustrated diameter ranging from 30 - 35 nm, where the average diameter of NFC/Gly-CA is 30.6 ± 5 nm and for NFC/Xyl-CA is 34.2 ± 5 nm while length is in micrometre range, thereby indicating a high efficiency of nanofibrillation. The obtained result demonstrated that the samples consisted several larger bundles of NFCs and irregular aggregates. These alterations in fibre size and structure observed after different pretreatment and high intensity ultrasonication might be attributed to the hydrolysis and cleavage of

glycosidic linkages in LCB. The results obtained were in agreement with DLS analysis of NFC samples. Based on these apparent observations, it can be inferred that cellulose fibrillation takes place through mechanisms that involve the fragmentation of larger bundles into smaller particles and the separation of individual nanofibrils from the surfaces of larger fibres.

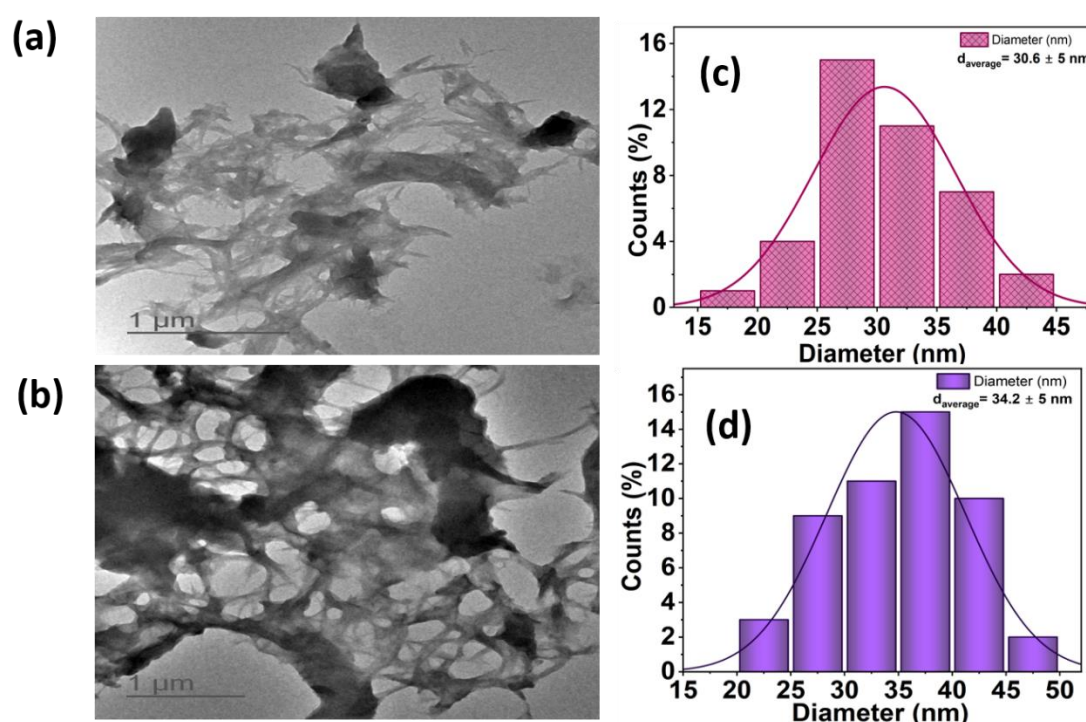


Figure 3.6 TEM images of (a) NFC/Gly-CA; (b) NFC/Xyl-CA; particle size distribution of (c) NFC/Gly-CA; (d) NFC/Xyl-CA.

3.6.6 Scanning Electron Microscopy and Energy-Dispersive X-ray Spectroscopy (SEM-EDS)

The morphological analysis of NFC samples (see Figure 3.7) revealed that cellulosic materials exhibit heterogeneity and irregularities with varying shapes and sizes [104]. Identifying similar structures at a specific magnification is challenging due to the heterogeneity in particle morphologies. However, the results clearly demonstrated that NFCs were significantly smaller compared to the untreated raw sample. As seen in

Figure 3.7 a, in the untreated sample, the fibres exhibited larger sizes, and were easily discernible at lower magnifications. Each fibre consisted of multiple microfibrils displaying a compact sheet structure and alignment along the axis of the fibre. Also, the micrograph of the untreated biomass sample exhibits a uniform and even surface without any noticeable distortions that maybe due to the presence of waxes and oil. In contrast, the synthesized NFCs (Figure 3.7 b and c) were considerably smaller in size, primarily displaying elongated fibrous structure, and were identifiable only at higher magnifications. The micrographs of NFCs as depicted in figures demonstrate significant refinement of the fibrillar structure, characterized by a reduction in diameter, intermittent disruptions in the axial direction of the fibrils and enhanced surface roughness resulting from the removal of non-cellulosic elements. These observations highlight the important aspects of pre-treatment as it plays a crucial role in swelling the fibres, facilitating the penetration of solvents (combined NADES and acetosolv) into the cementing matrix, thereby disintegrating the recalcitrant structure.

Energy Dispersive X-ray Spectroscopy (EDX) analysis of NFCs revealed the presence of carbon and oxygen peaks corresponding to their respective binding energies. Figure 3.7 d represents the elemental analysis of pristine biomass which is an indicative that pretreatment resulted in the removal or reduction of certain elements such as sodium, silicon, chlorine, magnesium, potassium and calcium, and other impurities as indicated by their decreased percentages. However, the composition of the synthesized NFCs majorly includes carbon, hydrogen, and oxygen elements (3.7 e and f). Due to the limitations of EDS analysis in detecting hydrogen, the results only depicted the percentages of carbon and oxygen. The EDS cartography of NFCs illustrates a higher percentage of carbon compared to oxygen. The third peak corresponds to gold, as the

samples, which were initially nonconducting, were sputtered with gold particles for SEM imaging. This finding aligns with typical characteristics of cellulose [185].

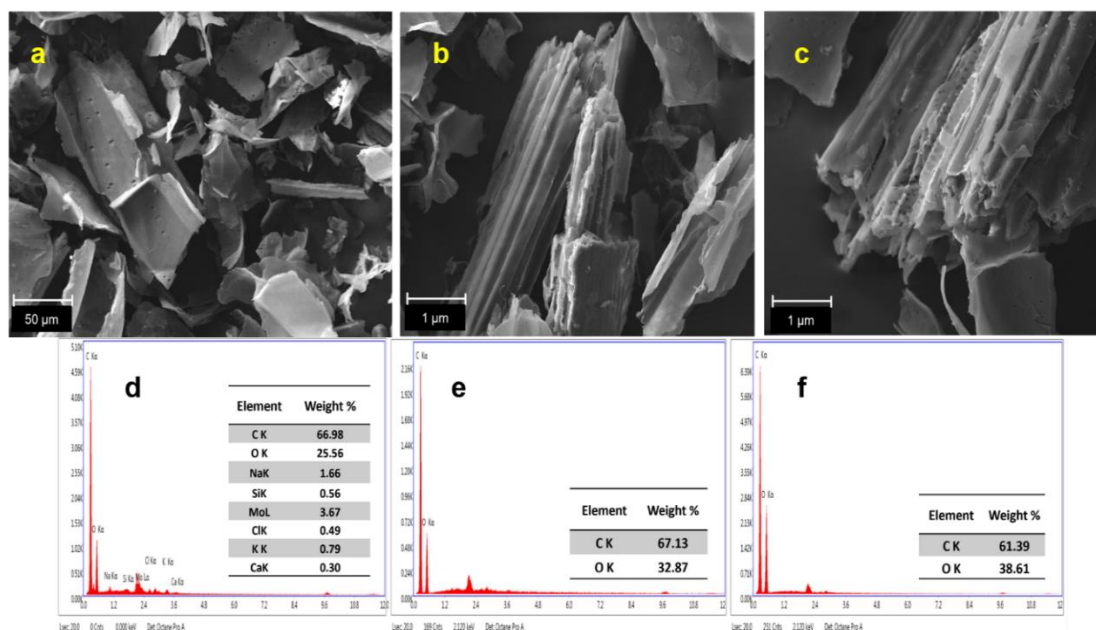


Figure 3.7 SEM images and EDX of (a & d) untreated biomass; (b & e) NFC/Gly-CA; (c & f) NFC/Xyl-CA respectively.

The approach outlined in this study gave interesting outcomes, allowing for a comparison of the extracted NFCs with those obtained in previous literatures, including feedstock, production method, nanocellulose yield, dimensions, CrI % of nanocellulose (as indicated in Table 3.2). According to the information, the predominant technique employed for producing nanocellulose was acid/alkali hydrolysis along with other assistive techniques. Despite similarities in feedstock composition (cellulose, hemicellulose and lignin), nanocellulose yield obtained through other methods was below 90% in all the cases, which was considerably lower than 95% achieved with our method. In general, the NFCs exhibited similar characteristics in terms of morphology, crystallinity, dimensions, and thermal stability as nanocelluloses produced through conventional methods. However, it is worth noting that the NFCs produced in our study

were more environmentally friendly, and the acid-catalyzed pretreatment demonstrated greater efficiency, resulting in a higher yield compared to other reported studies.

Table 3.2 A comparison table of feedstock used, production methods, nanocellulose yield, and its properties.

Feedstock	Methods of production	NC recovered (%)	Crystallinity (%)	Dimension	Reference
Sugarcane bagasse	<ul style="list-style-type: none"> Ultrasonic assisted NADES + acetosolv treatment 	95	64	length-25-80 nm	This study
Cotton fibres	<ul style="list-style-type: none"> Choline chloride + oxalic acid + high intensity ultrasonication Choline chloride + citric acid + high intensity ultrasonication 	65	93	length- 143 nm	[186]
Wheat cellulose	<ul style="list-style-type: none"> Ultrasonic-assisted enzymatic hydrolysis process 	22.57	≥80	width ≥10 nm length- 40-50 nm	[187]
Sugarcane bagasse	<ul style="list-style-type: none"> choline chloride: oxalic acid: $AlCl_3 \cdot 6H_2O$, and choline chloride: lactic acid: $AlCl_3 \cdot 6H_2O$, (molar ratio 1:1:0.2) 	56 and 63	58.05 and 60.71	length- 400-600 nm,	[149]
Kenaf fibres and wheat straw	<ul style="list-style-type: none"> organic acids (formic and acetic acid) and hydrogen peroxide followed by ball milling Wet method (10 mL of 80% ethanol/ water mixture) 	-	65 and 68	100 nm in range	[188]
Sugarcane bagasse	<ul style="list-style-type: none"> Alkali (NaOH) - acid (HCl) 	65	58.32	diameter- 57 nm	[189]

		<i>treatment followed by high-speed grinding at a revolution of 1500 rpm for 20 min</i>				
Short, medium and long grain rice husks	•	<i>Solvent extraction, alkali treatment, bleaching, ultrasonication</i>	34, 37, and 41	58.82, 62.32 and 76.69	lengths- 55-178 nm, 111 -476 nm and 153-778 nm	[190]
Culinary Banana Flower Waste	•	<i>Alkali (KOH) + ultrasonication</i>	89	67.76	-	[191]
Cotton fibres	•	<i>Microwave-assisted DES pretreatment and subsequent high-intensity ultrasonication process</i>	74.2	82	length- 100 - 350 nm	[192]

3.7 Conclusion

The study advocated sustainable and cleaner production of NFCs from SCB in a consecutive two-stage process involving the utilization of green and reusable solvents and HIU. Synthesis of acidic NADES and their structural properties were compared and evaluated through FTIR and NMR analysis. Gly-CA NADES combined with acetsov resulted in the maximum solubilization of hemicellulose and lignin respectively, without much loss in cellulose. The experiment brought about a considerable yield of 84.4 % of cellulose from SCB. NFC production (≥ 90 %) was accelerated by using HIU that helped in successful disintegration of all the extracted cellulosic fibres. Removal of hemicellulose and lignin was confirmed by FT-IR analysis. The morphological, structural and functional analysis of NFC samples correlated well with studies reported elsewhere. Further, DLS studies were in

agreement with SEM and TEM results of the particles. In addition, NFCs analysed with SEM-EDX, XRD and TGA/DTG elucidated the chemical composition and purity of the sample.

Additionally, the use of residual particles like hemicellulose and lignin in biorefinery technique may help the sugarcane processing business in capitalizing exceptionally. Thus, the work highlights the potential of transforming an agricultural residue, sugarcane bagasse into a high-value materials using environmentally benign and efficient methods, contributing to the broader goals of circular bioeconomy and sustainable material development.